Robotica (2010) volume 28, pp. 413–425. © Cambridge University Press 2009
doi:10.1017/S0263574709005736

Passive dynamic walking with flat feet and ankle compliance

Qining Wang†,‡*, Yan Huang†,‡ and Long Wang†,‡

†*Intelligent Control Laboratory, Center for Systems and Control, Department of Mechanics and Aerospace Engineering, Peking University, Beijing 100871, China*
‡*Key Laboratory of Machine Perception (Ministry of Education), Peking University, Beijing 100871, China*

(Received in Final Form: April 15, 2009. First published online: May 22, 2009)

SUMMARY
This paper presents a bipedal locomotion model for passive dynamic walking with flat feet and compliant ankles. The two-dimensional seven-link model extends the simplest walking model with the addition of hip actuation, knee joints, flat feet and torsional springs based compliance on ankle joints, concerning heel-strike and toe-strike transitions, to achieve adaptive bipedal locomotion on level ground with controllable walking speed. We investigate the effects of foot geometric parameters and ankles stiffness on bipedal walking. The model achieves satisfactory walking results not only on even ground but also on uneven terrain with no active control and on different walking velocities. In addition, from the view of stability, there is an optimal foot-ankle ratio of the passivity-based walker. The results can be used to explore further understanding of bipedal walking, and help the design of future intelligent ankle-foot prosthesis and passivity-based robot prototypes towards more practical uses.

KEYWORDS: Passive dynamic walking; Biped; Flat foot; Ankle compliance; Locomotion.

1. Introduction

Passive dynamic walking[1] has been developed as a possible explanation for the efficiency of the human gait, which showed that a mechanism with two legs can be constructed so as to descend a gentle slope with no actuation and no active control. The mechanical energy consumption of such a mechanism may be compensated by two kinds of actuation in the case of level ground walking: apply an impulsive push along the trailing leg or apply a hip torque against the stance leg. Several studies reported that these kinds of walking machines work with reasonable stability over a range of slopes[1,3,20] and on level ground with kinds of actuation added[4,6,10] show a remarkable resemblance to the human gait. In spite of having high efficiency of energetic cost and fast walking, passive dynamic walkers have several limits, such as controlling the start and stop of walking, actively changing the velocity during walking and autonomous locomotion on rough terrains.

Although passive dynamic walking models do not predict control strategies, the role of muscles and nerves in human walking may be better determined by first understanding how the system works without any sort of control.[13] Most studies of passive dynamic walking are based on the simplest walking model proposed by Garcia *et al.*[11] and extended work by Kuo,[14] which consist of two rigid massless legs connected by a frictionless hinge at the hip, with a large point mass at the hip and a small mass at each foot (placed at the ankle). Recently, a passive dynamic walking model with upper body has been proposed by Wisse *et al.*[5] In these models, passive walkers are often modelled with point feet or round feet which have clear disadvantages of being unable to achieve the start and stop of walking. However, only a few studies have been done on a flat foot shape in passive dynamic models.[2,12,15] These studies proposed that the flat foot with a geometric parameter (foot length) can introduce a toe-strike collision in addition to the heel-strike impulse and influence the passive dynamics of walking. It has been investigated that flat feet can distribute the energy loss per step over two collisions, at the heel and at the toe. In addition, compliant ankles have been added to passive dynamic walkers.[7,8] The mechanical energy stored in such elastic elements can be recovered as both kinetic and gravitational energy. It may improve the efficiency and adaptability of bipedal walking. However, in these studies, the walker is modelled as a simple point foot model with a torsional spring between the stance leg and the floor. The effects of heel-strike and toe-strike during normal walking are ignored, which may influence the characteristics of bipedal walking.[15] Recent study on actuated limit cycle walkers reported that different control schemes of ankle actuation influence both the energy use and the disturbance rejection of the walkers.[9] Dynamic walking models with flat feet and passive ankle springs can largely resemble real human walking.

In this research, we extend the simplest walking model with the addition of hip actuation, upper body, flat feet and linear torsional springs based stiffness on ankle joints, aiming for adaptive bipedal locomotion in view of stability and efficiency. The goal of this study is to present a powered walking model with flat feet and compliant ankles, and to investigate the effects of the foot geometric parameters (foot length and foot-ankle ratio) and ankle stiffness on the walking characteristics. We divide one walking step into seven events, with specific analysis of heal-strike and toe-strike during dynamic walking. Based on the theoretical model, we first examine the performance of simulated walking on level

* Corresponding author. E-mail: qiningwang@pku.edu.cn

https://doi.org/10.1017/S0263574709005736 Published online by Cambridge University Press

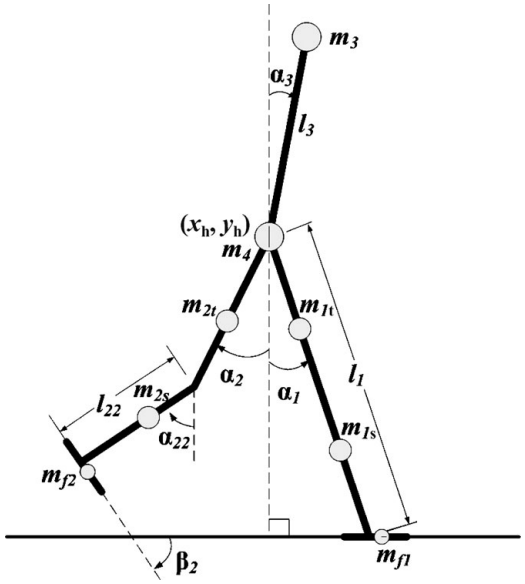


Fig. 1. Dynamic walking model of the simplest walker with upper body, flat feet and ankle stiffness. Mechanical energy consumption of level ground walking is compensated by applying a hip torque. The global coordinates of the hip joint is notated as (x_h, y_h). α_1 and α_2 are the angles between each leg and the vertical axis in sagittal plane respectively. The ankle joints are passive joints constrained by torsional springs. The positive direction of $\alpha_1, \alpha_2, \beta_1, \beta_2$ are counter-clockwise while the positive direction of α_{11}, α_{22} are clockwise. The x-axis is along the level ground while the y-axis is vertical to the ground upwards.

ground and actively changing walking speed during stable walking. Second, we study the dynamic stability of the walker. Then the effects of ankle stiffness and flat feet on passivity-based bipedal walking are investigated.

This paper is organized as follows. Section 2 describes the passive dynamic walking model with flat feet and compliant ankles in detail. In Section 3, we show the walking results of the proposed model. In section 4, we discuss the effects of the foot geometric parameters and ankle stiffness on the walking characteristics. We conclude in Section 5.

2. Model

This research extends the simplest walking model with the addition of hip actuation, flat feet and compliant ankles. Our model consists of an upper body (point mass added stick) that rotates around the hip joint, a point mass representing the pelvis, two legs with knee joints and ankle joints, and two mass-added flat feet (see Fig. 1). The mass of each leg is simplified as point masses added on the Centre of Mass (CoM) of the shank and the thigh, respectively. Note that for the purpose of achieving controllable velocity of walking, we use hip actuation as a numerical torque instead of the 'hip spring stiffness' which is normally used in the existing models.[14,5] In addition, our model added compliance to the ankle joints. Specifically, the ankle joints are modelled as passive joints that are constrained by linear torsional springs. If the foot has no contact with the ground, the torsional spring on the ankle will constraint the foot vertically to the shank. Additionally, the knee will lock the shank when the shank and the thigh keep in a straight line. Similar to the model proposed by Wisse *et al*,[5] a kinematic coupling has been used in the proposed model to keep the body midway between the two legs (say $\alpha_3 = \frac{1}{2}(\alpha_1 + \alpha_2)$). The default parameter values in the following analysis are shown in Table I, which are obtained from our previous robot prototype.[24] c_b is the distance between hip joint and CoM of upper body. c_1 and c_2 represent the distance between hip joint and CoM of each thigh respectively. c_{11} and c_{22} represent the distance between knee joint and CoM of each shank, respectively. The flat foot shape can be simply defined by two parameters, foot length l_f and foot-ankle ratio r (distance from heel to ankle/foot length).

Table I. Default parameter values for the dynamic walking model and the following simulations.

Parameter	Value	Parameter	Value
Upper body mass m_3	0.81 kg	Upper body length l_b	0.5 m
Hip mass m_4	15.03 kg	CoM of upper body c_b	0.2 m
Leg mass m_1, m_2	1.12 kg	CoM of leg c_1, c_2	0.2 m
Thigh mass m_{1t}, m_{2t}	0.56 kg	CoM of shank c_{11}, c_{22}	0.2 m
Shank mass m_{1s}, m_{2s}	0.56 kg	Ankle stiffness k	1.65 Nm/rad
Foot mass m_{f1}, m_{f2}	2.05 kg	Foot ratio r	0.33
Leg length l_1, l_2	0.7 m	Hip torque p	0.38 Nm
Foot length l_{f1}, l_{f2}	0.15 m	Shank length l_{11}, l_{22}	0.35 m

Here, the two-dimensional model has some assumptions as follows:

- Shanks and thighs suffer no flexible deformation during locomotion.
- There is no damping or friction on the hip joint.
- Flat feet do not deform or slip during locomotion, even on uneven terrain.
- Heel-strike and toe-strike are modelled as an instantaneous, fully inelastic impact where no slip and no bounce occurs.

The passive walker travels forward on level ground. The stance leg keeps contact with the ground while the swing leg pivots about the constraint hip. To compensate the mechanical energy consumption, similar to the Powered Walking Model,[14] we added a hip torque between the swing leg and the stance leg. The hip torque is constant during simulated walking. When the flat foot strikes the ground, there are two impulses, 'heel-strike' and 'toe-strike', representative of the initial impact of the heel and the following impact as the whole foot contact the ground. Note that actually when the shank swings (α_1 or α_2 varies), the moment of inertia of the leg changes. However, since the swing angle of the shank is relatively small and the time duration of large swing angle is quite short, we simplified the moment of inertia of the leg as a constant. Additionally, the springs on the compliant ankles constrain the foot vertical to the shank when no heel-strike or toe-strike has occurred.

https://doi.org/10.1017/S0263574709005736 Published online by Cambridge University Press

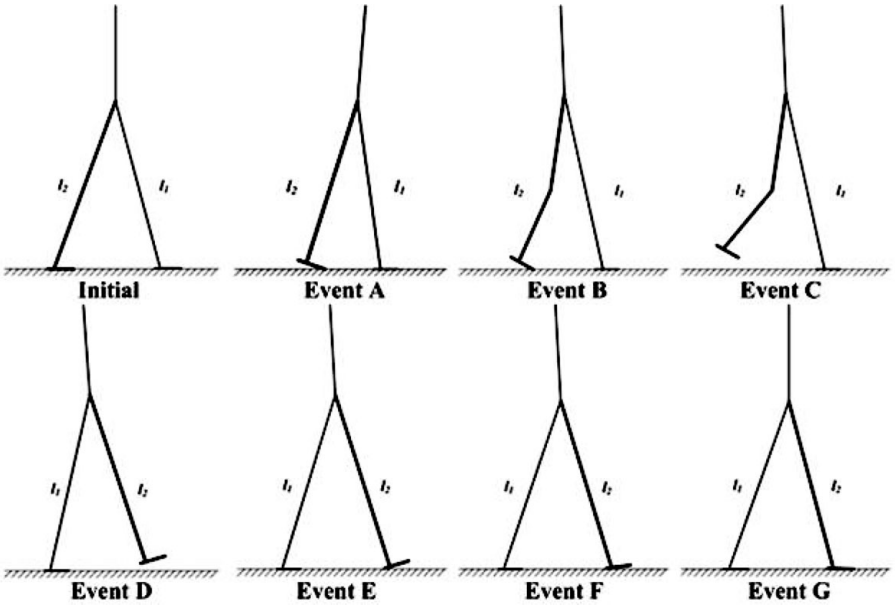


Fig. 2. The event sequence of one walking step.

2.1. Walking events

In this study, we describe one walking step with specification of seven events (see Fig. 2). The model can be defined by the rectangular coordinates x which can be described by the x-coordinates and y-coordinates of the mass points and the corresponding angles. The walker can also be described by the generalized coordinates q. Note that in different walking phases, the specific components of x and q may be different.

Event A. Suppose that leg 1 (l_1) is the stance leg, while leg 2 (l_2) is the swing leg. The knee joint is locked (keep the shank and the thigh in a straight line). In this phase, the foot of leg 2 rotates around the ankle joint. The stance leg maintains foot contact with ground and the swing leg maintains toe contact with ground. Since the foot rotates around the ankle joint and we pay special attention to the relative motion of the foot, the swing leg can not be studied as a whole object. Consequently, the foot of the swing leg (l_2) is not included in the objects of study and the force generated by the springs on the swing leg should be considered as external force. Suppose that the friction force of the ground is big enough that the toe of the swing leg (l_2) is a contact point with no slip. Then the foot of leg 2 rotates around a fixed point (the toe of the foot) in this phase. And we can consider that the ankle joint of the swing leg (l_2) is constrained to move in a circular orbit with toe as the centre and distance between toe and ankle joint as the radius.

During this phase, since the knee is locked, the walker can be described by the rectangular coordinates x and the generalized coordinates q as follows:

$$x = [x_{m1} \quad y_{m1} \quad \alpha_1 \quad x_{m2} \quad y_{m2} \quad \alpha_2 \quad x_{m3} \quad y_{m3} \quad \alpha_3 \quad x_{m4} \quad y_{m4}]^T, \tag{1}$$

$$q = [x_{\mathrm{h}} \quad y_{\mathrm{h}} \quad \alpha_1 \quad \alpha_2]^T. \tag{2}$$

The constraint equations ξ_1, ξ_2, ξ_3 and ξ_4 used in this event are:

$$\begin{aligned}
\xi_1 &= \begin{bmatrix} x_{\mathrm{h}} + l_1 \sin\alpha_1 - x_{\mathrm{a1}} \\ y_{\mathrm{h}} - l1 \cos\alpha_1 \end{bmatrix}, \\
\xi_2 &= \begin{bmatrix} x_{\mathrm{h}} + l_2 \sin\alpha_2 - x_{\mathrm{a2}} \\ y_{\mathrm{h}} - l2 \cos\alpha_2 \end{bmatrix}, \\
\xi_3 &= [x_{\mathrm{h}} + l_1 \sin\alpha_1 - x_{t1}]^2 + [y_{\mathrm{h}} - l_1 \cos\alpha_1]^2 - l_{f11}^2, \\
\xi_4 &= [x_{\mathrm{h}} + l_2 \sin\alpha_2 - x_{t2}]^2 + [y_{\mathrm{h}} - l_2 \cos\alpha_2]^2 - l_{f21}^2,
\end{aligned} \tag{3}$$

where x_{a1} and x_{a2} are the global x-coordinates of the latest foot strike (the x-coordinates of the ankles) of leg 1 and leg 2, while x_{t1} and x_{t2} are the global x-coordinates of the toes of leg 1 and leg 2. l_{f11} and l_{f21} are the distances between the ankle joint and the toe of leg 1 and leg 2. When the flat foot completely contacts the ground, the constraint equations ξ_1 and ξ_2 used to maintain foot contact with ground. ξ_3 and ξ_4 are used to constrain the ankle joint to move in the circular orbit mentioned above.

Matrix $\sum_i$ transfers the independent generalized coordinates q into the constraint equation ξ_i, where $i = 1, 2, \ldots, 6$:

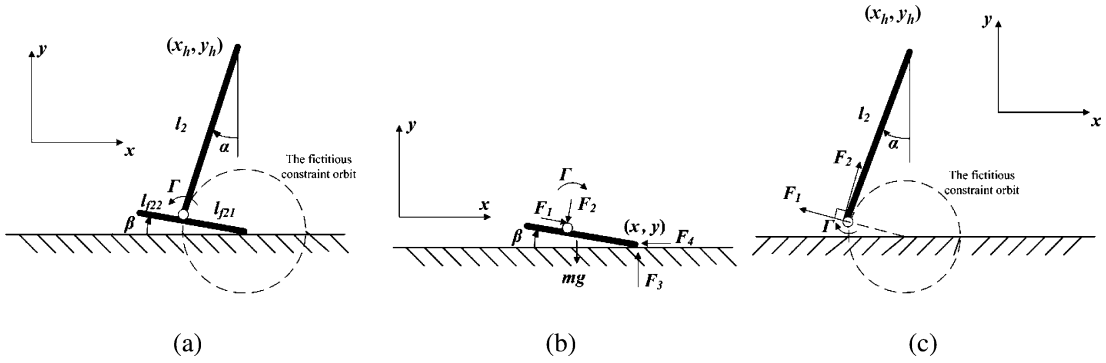
$$\sum\nolimits_i = \frac{\mathrm{d}\xi_i}{\mathrm{d}q}. \tag{4}$$

Consequently, matrix Ψ_i is defined as follows:

$$\Psi_i = \frac{\partial\left(\sum_i \dot{q}\right)}{\partial q}\dot{q}. \tag{5}$$

Then we can obtain the Equation of Motion(EoM) in this state by the principle of virtual work (suppose that leg 1 is the stance leg while leg 2 is the swing

https://doi.org/10.1017/S0263574709005736 Published online by Cambridge University Press



(a) (b) (c)

Fig. 3. Analysis of the external force in Event A.

leg):

$$\begin{bmatrix} M_r & \sum_1^T & \sum_4^T \\ \sum_1 & 0 & 0 \\ \sum_4 & 0 & 0 \end{bmatrix} \begin{bmatrix} \ddot{q} \\ F_1 \\ F_4 \end{bmatrix} = \begin{bmatrix} F_r \\ -\Psi_1 \\ -\Psi_4 \end{bmatrix}, \tag{6}$$

where $\ddot{q}$ is the acceleration in the generalized coordinate. M_r is a reduced mass matrix:

$$[M_r] = [T]^T [M][T]. \tag{7}$$

Here matrix T, which can be described by $T = \mathrm{d}q/\mathrm{d}x$, transfers the independent generalized coordinates $\dot{q}$ into the velocities of the mass points $\dot{x}$. And F_r is the external force in generalized coordinates which is defined as follows:

$$\{F_r\} = [T]^T (\{F\} - [M]\{\ddot{x}\}). \tag{8}$$

Here F is the active external force. Note that the corresponding mass matrix in the rectangular coordinate M does not include the mass of the foot of swing leg as we described above. F_1 is the force acted on the ground by the stance leg, while F_4 is the force acted on the constraint circular orbit described by ξ_4.

As we mentioned above, the force generated by the spring on the swing leg should be considered as external force. Consequently, in this event, f_c includes the force and the torque that acts on the swing leg, which are provided by the respective foot (it can also be considered as the constraint force of the circular orbit) and the torque provided by the compliant ankle acting on the stance leg. Suppose that leg 1 is the stance leg and leg 2 is the swing leg, then we can obtain the force as follows:

$$f_c = [0 \quad 0 \quad T_1 \quad f_x \quad f_y \quad T_2 \quad 0 \quad 0 \quad 0 \quad 0 \quad 0]^T, \tag{9}$$

where T_1 and T_2 are the torques acting on the leg 1 and leg 2 as a result of the compliant ankle joint. f_x and f_y are the force acting on the swing leg in the orientation of x-axis and y-axis. The torques are

$$T_1 = -k\alpha_1. \tag{10}$$

Since the swing leg is supposed to move on a circular surface, F_1 and F_2 (see Fig. 3), generated by the foot, are considered as the constraint force provided by the constraint surface. F_1 is the normal force while F_2 is the tangential force. F_1 can be considered as constraint force, while F_2 is active force which should be included in f_c, the circular surface can be considered as an ideal constraint consequently. Suppose that the global coordinates of the ankle joint is (x_a, y_a), the x-coordinate of the toe is $(x_t, 0)$ and k is the spring constant for the ankle joint spring. Note that $\beta = -\beta_2$ and $\alpha = -\alpha_2$ here.

The EoM of the foot can be described as follows:

$$I_{f2}\ddot{\beta} = -mgl_{f2}\cos\beta - F_2 l_{f21} + k(\alpha - \beta), \tag{11}$$

where l_{f2} is a half length of the foot. From Eq. (11), we can obtain the active force F_2:

$$F_2 = \frac{1}{l_{f21}}[k(\alpha - \beta) - mgl_{f2}\cos\beta - I_{f2}\ddot{\beta}]. \tag{12}$$

Then we can write the external force as follows:

$$f_x = F_2 \sin\beta = \frac{y_a}{l_{f21}^2}\left[k(\alpha - \beta) - mg\frac{l_{f2}}{l_{f21}}(x_t - x_a) - I_{f2}\ddot{\beta}\right], \tag{13}$$

$$f_y = F_2 \cos\beta = \frac{x_t - x_a}{l_{f21}^2}\left[k(\alpha - \beta) - mg\frac{l_{f2}}{l_{f21}}(x_t - x_a) - I_{f2}\ddot{\beta}\right]. \tag{14}$$

The torque acted on the leg is

$$T_2 = \Gamma = k(\alpha - \beta). \tag{15}$$

According to the kinematic constraint $\beta = arctan\frac{y_t}{x_t - x_a}$, we can obtain $\ddot{\beta}$:

$$\ddot{\beta} = \frac{l_2}{l_{f21}}\cos\left(\alpha_2 + arctan\frac{y_a}{x_t - x_a}\right)\dot{\alpha_2}^2 + \frac{y_a}{l_{f21}^2}\ddot{x_h} + \frac{x_t - x_a}{l_{f21}^2}\ddot{y_h}. \tag{16}$$

From Eq. (16), we can have f_x, f_y and T_2 which should be included in the active external force F_r. And the EoM of this phase can be solved.

When the knee joint releases the shank, the model moves to Event B.

https://doi.org/10.1017/S0263574709005736 Published online by Cambridge University Press

Event B. Leg 1 (l_1) is still the stance leg, while leg 2 keeps swinging. In this phase, the knee joint releases the shank, which is the only difference between Event B and Event A.

The constraint equation of the swing leg is changed to

$$\begin{aligned}\tilde{\xi}_3 &= [x_\mathrm{h} + (l_1 - l_{11})\sin\alpha_1 + l_{11}\sin(\alpha_1 - \alpha_{11}) - x_{\mathrm{t}1}]^2 \\ &\quad + [y_\mathrm{h} - (l_1 - l_{11})\cos\alpha_1 - l_{11}\cos(\alpha_1 - \alpha_{11}))]^2 - l_{\mathrm{f}11}^2, \\ \tilde{\xi}_4 &= [x_\mathrm{h} + (l_2 - l_{12})\sin\alpha_2 + l_{22}\sin(\alpha_2 - \alpha_{22}) - x_{\mathrm{t}2}]^2 \\ &\quad + [y_\mathrm{h} - (l_2 - l_{22})\cos\alpha_2 - l_{22}\cos(\alpha_2 - \alpha_{22}))]^2 - l_{\mathrm{f}21}^2.\end{aligned} \tag{17}$$

Here $\tilde{\xi}_3, \tilde{\xi}_4$ are the same with ξ_3, ξ_4 when α_{11}, α_{22} are restricted to be zero. The constraint equations are still ξ_1 and ξ_2.

The EoM of the model in this event can be described as follows:

$$\begin{bmatrix} M_r & \sum_1^T & \sum_4^T \\ \sum_1 & 0 & 0 \\ \sum_4 & 0 & 0 \end{bmatrix} \begin{bmatrix} \ddot{q} \\ F_1 \\ F_4 \end{bmatrix} = \begin{bmatrix} F_r \\ -\Psi_1 \\ -\Psi_4 \end{bmatrix}. \tag{18}$$

Note that since the constraint equation changes, the EoM is different from Eq. (6). Here, since the knee is unlocked, the number of components of x and q increases. The specific components of x and q are different from Eqs. (19) and (20):

$$\begin{aligned} x = [&x_{m1} \quad y_{m1} \quad \alpha_1 \quad x_{m2\mathrm{t}} \quad y_{m2\mathrm{t}} \quad \alpha_2 \quad x_{m2\mathrm{s}} \\ &y_{m2\mathrm{s}} \quad \alpha_{22} \quad x_{m3} \quad y_{m3} \quad \alpha_3 \quad x_{m4} \quad y_{m4}]^T, \end{aligned} \tag{19}$$

$$q = [x_\mathrm{h} \quad y_\mathrm{h} \quad \alpha_1 \quad \alpha_2 \quad \alpha_{22}]^T, \tag{20}$$

where α_{22} is the angle between thigh and shank of the swing leg.

It is clear that Event A can be considered as a particular case of Event B. The time of shank swing can be adjusted to obtain a satisfied walking. When the direction of F_1 acting on the leg points to the toe (the centre of the frictions constraint surface), the swing leg is considered to leave the frictions constraint surface, which means the foot is out of contact with the ground. Then the model moves to Event C.

Event C. Leg 1 is the stance leg, while leg 2 swings freely and the shank is released. The springs on the compliant ankle of the swing leg constrains the foot vertical to the shank. The EoM of the model in this phase is

$$\begin{bmatrix} M_r & \sum_1^T \\ \sum_1 & 0 \end{bmatrix} \begin{bmatrix} \ddot{q} \\ F_1 \end{bmatrix} = \begin{bmatrix} F_r \\ -\Psi_1 \end{bmatrix}. \tag{21}$$

Note that the number of the components of M_r, q, and f_r increases. Since leg 2 swings freely, f_c includes only T_1 in this phase. When the leg 2 has passed mid-stance and the shank swings to a relatively small angle, the knee is locked and the model moves to Event D.

Event D. This event starts when the knee is locked. From the impact occurring due to knee-strike, we can have the following equations:

$$\begin{aligned}\overrightarrow{L_A^-} &= I_1\dot{\alpha}_1^-\vec{k} + \overrightarrow{AC} \times m_1\overrightarrow{v_{c1}^-} + I_{2\mathrm{t}}\dot{\alpha}_2^-\vec{k} + \overrightarrow{AC_{2\mathrm{t}}} \times m_{2\mathrm{t}}\overrightarrow{v_{c2\mathrm{t}}^-} \\ &\quad + I_{2\mathrm{s}}\dot{\alpha}_{22}^-\vec{k} + \overrightarrow{AC_{2\mathrm{s}}} \times m_{2\mathrm{s}}\overrightarrow{v_{2\mathrm{s}}^-} + I_3\dot{\alpha}_3^-\vec{k} \\ &\quad + \overrightarrow{AC_3} \times m_3\overrightarrow{v_3^-} + I_{2\mathrm{f}}\dot{\alpha}_{22}^-\vec{k} + \overrightarrow{AC_{2\mathrm{f}}} \times m_{2\mathrm{s}}\overrightarrow{v_{2\mathrm{f}}^-}, \\ \overrightarrow{L_A^+} &= I_1\dot{\alpha}_1^+\vec{k} + \overrightarrow{AC} \times m_1\overrightarrow{v_{c1}^+} + I_2\dot{\alpha}_2^+\vec{k} + \overrightarrow{AC_2} \times m_2\overrightarrow{v_2^+} \\ &\quad + I_3\dot{\alpha}_3^+\vec{k} + \overrightarrow{AC_3} \times m_3\overrightarrow{v_3^+} + I_{2\mathrm{f}}\dot{\alpha}_2^+\vec{k} + \overrightarrow{AC_{2\mathrm{f}}} \times m_{2s}\overrightarrow{v_{2\mathrm{f}}^+}, \\ \overrightarrow{L_H^-} &= I_{2\mathrm{t}}\dot{\alpha}_2^-\vec{k} + \overrightarrow{HC_{2\mathrm{t}}} \times m_{2\mathrm{t}}\overrightarrow{v_{c2\mathrm{t}}^-} + I_{2\mathrm{s}}\dot{\alpha}_{22}^-\vec{k} \\ &\quad + \overrightarrow{HC_{2\mathrm{s}}} \times m_{2\mathrm{s}}\overrightarrow{v_{c2\mathrm{s}}^-} + I_{2\mathrm{f}}\dot{\alpha}_{22}^-\vec{k} + \overrightarrow{HC_{2\mathrm{f}}} \times m_{2\mathrm{f}}\overrightarrow{v_{2\mathrm{f}}^-}, \\ \overrightarrow{L_H^+} &= I_2\dot{\alpha}_2^+\vec{k} + \overrightarrow{HC_2} \times m_2\overrightarrow{v_{c2}^+} + I_{2\mathrm{f}}\dot{\alpha}_{22}^+\vec{k} + \overrightarrow{HC_{2\mathrm{f}}} \times m_{2\mathrm{f}}\overrightarrow{v_{2\mathrm{f}}^+},\end{aligned} \tag{22}$$

with $\dot{\alpha}_1^-$ and $\dot{\alpha}_{22}^-$ the velocities before and $\dot{\alpha}_1^+$ and $\dot{\alpha}_2^+$ the velocities after the impact. $\vec{k}$ is the unit vector vertical to the motion plane. A is the contact point of the stance leg (ankle), while H is the point of the hip joint. C_1 and C_2 are the points of the CoM of the stance leg and the swing leg, respectively. $C_{2\mathrm{t}}$ and $C_{2\mathrm{s}}$ are the points of the CoM of the thigh and the shank of the swing leg, respectively. By the law of conservation of moment of momentum, we can obtain $\overrightarrow{L_A^-} = \overrightarrow{L_A^+}$ and $\overrightarrow{L_H^-} = \overrightarrow{L_H^+}$ from Eq. (22) to calculate the velocities after the impact, $\dot{\alpha}_1^+$ and $\dot{\alpha}_2^+$.

Then leg 2 swings freely. The EoM of the model is still Eq. (21) and f_c includes only T_1. If the heel contacts the ground, the model moves to Event E.

Event E. In this phase, the heel contacts the ground (heel-strike-occurs). The constraint equations in this phase are

$$\begin{aligned}\xi_5 &= \begin{bmatrix} x_\mathrm{h} + l_1\sin\alpha_1 - l_{\mathrm{f}12}\cos\alpha_1 - x_{\mathrm{he}1} \\ y_\mathrm{h} - l_1\cos\alpha_1 - l_{\mathrm{f}12}\sin\alpha_1 \end{bmatrix}, \\ \xi_6 &= \begin{bmatrix} x_\mathrm{h} + l_2\sin\alpha_2 - l_{\mathrm{f}22}\cos\alpha_2 - x_{\mathrm{he}2} \\ y_\mathrm{h} - l_2\cos\alpha_2 - l_{\mathrm{f}22}\sin\alpha_2 \end{bmatrix},\end{aligned} \tag{23}$$

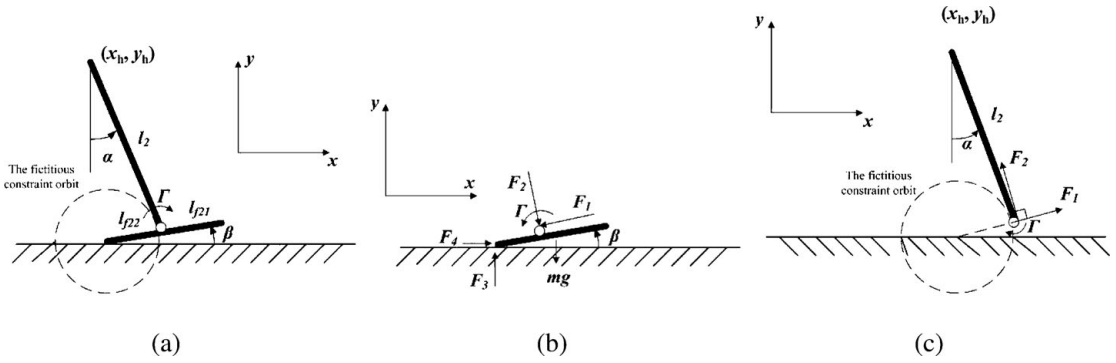
where $x_{\mathrm{he}1}$ and $x_{\mathrm{he}2}$ are the x-coordinates of the heel of leg 1 and leg 2. The impact equation of the model changes to

$$\begin{bmatrix} M_r & \sum_6^T \\ \sum_6 & 0 \end{bmatrix} \begin{bmatrix} \dot{q}^+ \\ F_6 \end{bmatrix} = \begin{bmatrix} M_r\dot{q}^- \\ -e\sum_6\dot{q}^- \end{bmatrix}, \tag{24}$$

where $\sum_6 = \frac{\mathrm{d}\xi_6}{\mathrm{d}q}$, $\dot{q}^-$ and $\dot{q}^+$ are the velocities in the generalized coordinates before and after the heel-strike. And e is the collision coefficient. Since we assume the strike is a fully inelastic impact, e is zero in this model. F_6 is the force acting on the ground generated by the heel of leg 2. After the heel-strike, the model moves to Event F.

Event F. In this phase, the motion is similar to that in Event A. Leg 1 (l_1) is still the stance leg, while leg 2 (l_2) is the swing leg. The knee joint is locked. The foot of leg 2 rotates around the ankle joint. The swing leg maintains heel contact with ground. The foot of the swing leg (l_2) is not included of the objects of study and the force generated by the springs on the

https://doi.org/10.1017/S0263574709005736 Published online by Cambridge University Press



(a) (b) (c)

Fig. 4. Analysis of external force in Event F.

swing leg should be considered as external force. Suppose that the friction force of the ground is big enough that the heel of the swing leg (l_2) is a contact point with no slip. The foot of leg 2 rotates around a fixed point (the heel of the foot) in this phase. And we can consider that the ankle joint of the swing leg (l_2) is constrained to move in a circular orbit with heel as the centre and distance between heel and ankle joint as the radius (see Fig. 4).

The constraint equations ξ_7 and ξ_8 used instead of ξ_3 and ξ_4 in this phase are

$$\begin{aligned}\xi_7 &= [x_\mathrm{h} + l_1 \sin\alpha_1 - x_{\mathrm{he}1}]^2 + [y_\mathrm{h} - l_1 \cos\alpha_1]^2 - l_{\mathrm{f}12}^2,\\ \xi_8 &= [x_\mathrm{h} + l_2 \sin\alpha_2 - x_{\mathrm{he}2}]^2 + [y_\mathrm{h} - l_2 \cos\alpha_2]^2 - l_{\mathrm{f}22}^2,\end{aligned} \tag{25}$$

where $x_{\mathrm{he}1}$ and $x_{\mathrm{he}2}$ are the global x-coordinates of the heels of leg 1 and leg 2. $l_{\mathrm{f}12}$ and $l_{\mathrm{f}22}$ are the distances between the ankle joint and the heel of leg 1 and leg 2. ξ_7 and ξ_8 are used to constrain the ankle joint to move in the circular orbit mentioned above in this phase.

Matrix $\sum_i$ is still defined as follows:

$$\sum\nolimits_i = \frac{\mathrm{d}\xi_i}{\mathrm{d}q}. \tag{26}$$

Consequently, matrix Ψ_i is defined as follows:

$$\Psi_i = \frac{\partial\left(\sum_i \dot{q}\right)}{\partial q}\dot{q}. \tag{27}$$

The EoM of the model in this state is

$$\begin{bmatrix} M_r & \sum_1^T & \sum_8^T \\ \sum_1 & 0 & 0 \\ \sum_8 & 0 & 0 \end{bmatrix}\begin{bmatrix}\ddot{q}\\ F_1\\ F_8\end{bmatrix} = \begin{bmatrix} F_r \\ -\Psi_1 \\ -\Psi_8\end{bmatrix}. \tag{28}$$

The corresponding mass matrix in the rectangular coordinate M does not include the mass of the foot of swing leg as we described above. F_8 is the force acting on the constraint circular orbit described by ξ_8. And F_r is still the external force in generalized coordinates obtained by Eq. (8). The respective external force in rectangular coordinates includes gravity, hip torque(f) and f_c, produced by the compliant ankle joint. In this phase, f_c can be described by the Eq. (9). T_1 is the same with that in Event A. And we can obtain f_x, f_y and T_2 by the analysis of the force in the similar process:

Suppose that the global coordinates of the ankle joint is still $(x_\mathrm{a}, y_\mathrm{a})$, the x-coordinate of the heel is $(x_\mathrm{he}, 0)$ and k is the spring constant for the ankle joint spring. Note that $\beta = \beta_2$ and $\alpha = \alpha_2$ here. which is different from the case in Event A.

The EoM of the foot can be described as follows:

$$I_{\mathrm{f}2}\ddot{\beta} = -mgl_{\mathrm{f}2}\cos\beta - F_2 l_{\mathrm{f}22} + k(\alpha - \beta). \tag{29}$$

And we can obtain the active force F_2:

$$F_2 = \frac{1}{l_{\mathrm{f}22}}[k(\alpha-\beta) - mgl_{\mathrm{f}2}\cos\beta - I_{\mathrm{f}2}\ddot{\beta}]. \tag{30}$$

Then we can write the external force as follows:

$$\begin{aligned} f_x &= -F_2\sin\beta \\ &= -\frac{y_a}{l_{\mathrm{f}22}^2}\left[k(\alpha-\beta) - mg\frac{l_{\mathrm{f}2}}{l_{\mathrm{f}22}}(x_\mathrm{a} - x_\mathrm{he}) - I_{\mathrm{f}2}\ddot{\beta}\right], \end{aligned} \tag{31}$$

$$\begin{aligned} f_y &= F_2\cos\beta \\ &= \frac{x_\mathrm{a} - x_\mathrm{he}}{l_{\mathrm{f}22}^2}\left[k(\alpha-\beta) - mg\frac{l_{\mathrm{f}2}}{l_{\mathrm{f}22}}(x_\mathrm{a} - x_\mathrm{he}) - I_{\mathrm{f}2}\ddot{\beta}\right]. \end{aligned} \tag{32}$$

The torque acting on the leg is

$$T_2 = \Gamma = -k(\alpha - \beta). \tag{33}$$

According to the kinematic constraint $\beta = arctan\frac{y_\mathrm{a}}{x_\mathrm{a}-x_\mathrm{he}}$, we can obtain $\ddot{\beta}$:

$$\begin{aligned}\ddot{\beta} = &\frac{l_2}{l_{\mathrm{f}22}}\cos\left(\alpha_2 - arctan\frac{y_\mathrm{a}}{x_\mathrm{a}-x_\mathrm{he}}\right)\dot{\alpha}_2^2 \\ &+ \frac{y_\mathrm{a}}{l_{\mathrm{f}22}^2}\ddot{x}_\mathrm{h} + \frac{x_\mathrm{a}-x_\mathrm{he}}{l_{\mathrm{f}22}^2}\ddot{y}_\mathrm{h}.\end{aligned} \tag{34}$$

From Eq. (34), we can have f_x, f_y and T_2 which should be included in the active external force F_r. And the EoM of

https://doi.org/10.1017/S0263574709005736 Published online by Cambridge University Press

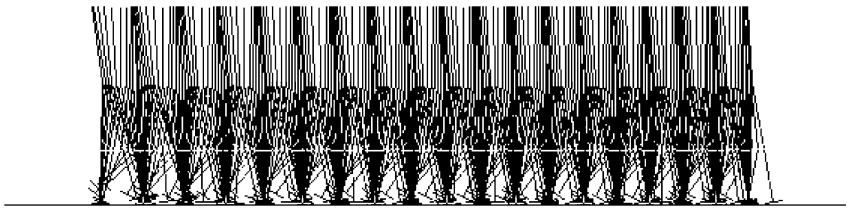


Fig. 5. Stable bipedal passive dynamic walking with flat feet and compliant ankles. The procedure of the simulation is a succession of nonlinear numerical dynamic simulations of walking steps which begin and end at the instant immediately after foot strike. Within one step, the EoM of the model are numerically integrated until one of the seven events is detected. After the toe-strike impact, one walking step is ended.

this phase can be solved. When the ankle joint contacts the ground, the model moves to Event G.

Event G. It is the toe-strike phase. The whole foot of the swing leg has an impact with the ground. The impact equation of the model is

$$\begin{bmatrix} M_r & \sum_2^T \\ \sum_2 & 0 \end{bmatrix} \begin{bmatrix} \dot{q}^+ \\ \tilde{F}_2 \end{bmatrix} = \begin{bmatrix} M_r \dot{q}^- \\ -e \sum_2 \dot{q}^- \end{bmatrix}. \tag{35}$$

where $\sum_2 = \frac{\mathrm{d}\xi_2}{\mathrm{d}q}$, $\dot{q}^-$ and $\dot{q}^+$ are the velocities in the generalized coordinates before and after the heel-strike. The collision coefficient e is still zero. $\tilde{F}_2$ is the force acting on the ground generated by the whole foot of leg 2. After the foot-strike, the model moves back to Event A. The stance leg and the swing leg will exchange the role in the next step.

In each state, falling down and running are detected. In Event D, shank releasing is detected and serious foot-scuffing is detected in both Event C and Event D. If these cases happen, the walker will be restricted to stop.

3. Results

3.1. Walking on level ground

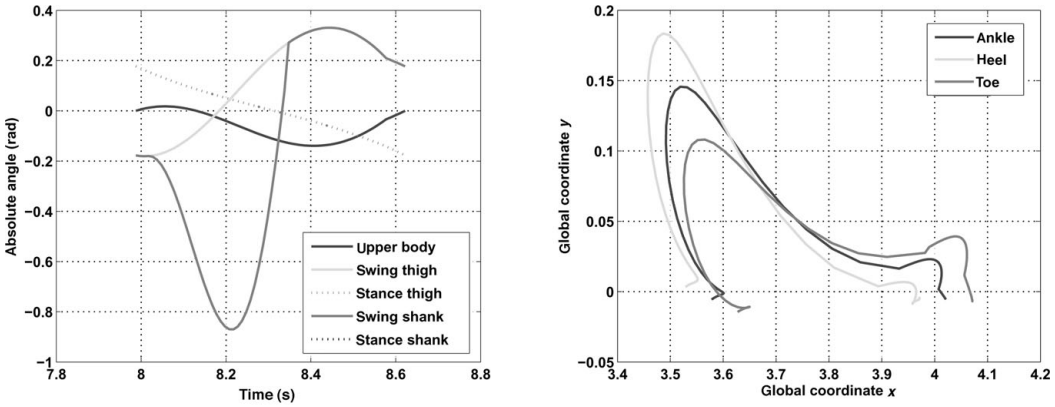
Based on the EoMs mentioned above, we analysed the walking motion of the proposed model on level ground. The numerical integration of the second-order differential EoMs uses the Runge–Kutta method, which is similar to the simulation methods used by Wisse *et al.*[5] In the simulations, the passive walking is restricted to stop in three cases, including falling down, running and shank releasing. We consider that the walker falls down if the angle of either leg exceeds the normal range. And the model is considered to running when all the forces act upwards on the walker provided by the floor. Shank releasing which means the shank of the swing leg is not locked before 'heel-strike'. Foot-scuffing, which often appears when the the knee joint locks the shank too early, is another case that the walker maybe have to stop. But this is likely avoided for a real three-dimensional walker with lateral motion, thus we allow this to happen if the foot travels below the floor not very seriously.

With the mechanical parameter values described in Table I, the model takes a stable bipedal waking step which shows a resemblance to the human gait (see Fig. 5). Since be more close to human characteristics, our model solved the typical non-human aspects of Garcia's simplest walking model[11] and Wisse's passive dynamic walking model with upper body.[5] First, the feet in the proposed model are flat, hence the heel-strike and toe-strike impulses, which are important in human walking gaits,[12,15] can be analysed. Second, the ankle stiffness simulates the tendons and muscles during walking, which are similar to real human walking step. Third, the hip joint actuation can power the model to walk on level ground, even on uneven terrain. Besides, the knee joints of the model can prevent from foot-scuffing when the swing leg passes the mid-stance.

The step starts and ends immediately after a toe-strike as described in Fig. 2. The hip torque actuates the pelvis to move forward like an inverted pendulum with controllable speed, while the swing leg swings to a forward position. It is predictable that one can control the hip actuation to change the velocity during walking. When the heel contacts the ground, the foot will rotate around the heel until the toe-strike impulse occurs. Figure 6 shows the trajectories of the different parts of the model. The trajectory of the hip is similar to the former results reported by Wisse *et al.*;[5,6] the hip moves forward on a circular path. It is clear that the stance thigh and the stance shank keep in a straight line during one step, since the knee locking mechanism. Thus, the absolute angles of them are equal in Fig. 6(a). From Fig. 6(a), one can also find that trajectory of the swing thigh coincides with the movement trace of the swing shank when the knee keeps locking, while the shank swings reversely to the thigh before mid-stance (in mid-stance, swing leg coincides with the stance leg) and then the shank and the thigh swing in the same direction on different angular speed, respectively. As observed by Kwan and Hubbard[15], Fig. 6(a) also indicates that the swing leg swings forward past the stance leg early in the walking cycle with an up-and-back swing into the heel-strike. This walking solution can be distinguished as a long-period solution which has slower steps but always stable. Figure 6(b) shows the trajectories of the heel, ankle and toe of the swing leg in one step. The trajectory of the foot during the seven events mentioned in Section 2 is clearly shown. Before the mid-stance, the foot is heading down (toe points the ground). Then the knee locks the shank and the heel points the ground. After heel-strike impulse, the foot rotates around the heel till toe-strike occurs. In the simulation, we defined the heel-strike and toe-strike impulses as the moment when the heel or toe travels below the floor level.

The energy consumption of passive dynamic based models is usually represented in the non-dimensional form of 'specific resistance': energy consumption per kilogram mass

https://doi.org/10.1017/S0263574709005736 Published online by Cambridge University Press



(a) (b)

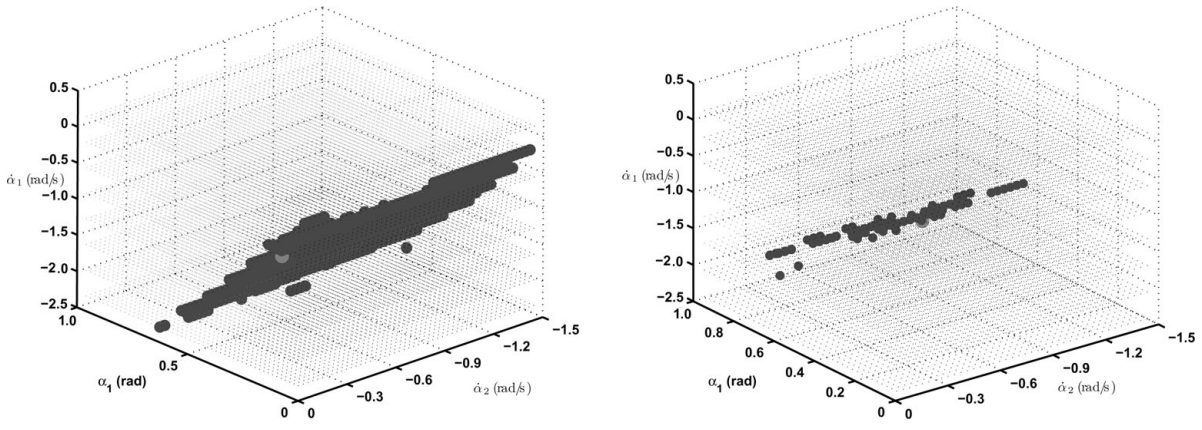
Fig. 6. Trajectories of different parts of the model in one step. The simulation is performed using the default parameter values in Table I. (a) shows the absolute angles of stance leg, swing thigh, swing shank, hip joint and upper body. (b) shows the trajectories of heel, ankle and toe of the swing leg.

per distance traveled per gravity.[4,5] By introducing flat feet and ankle stiffness, our model has a specific resistance of 0.065 at a scaled speed of 0.55 (walking speed/leg length). It is more efficient than not only the passive dynamic model with upper body,[5] but also human beings walking at the similar speed.[16]

Furthermore, the stability of the proposed model can be analysed by the approach of limit cycle analysis.[5] We found that the model with parameter values from Table I and a certain combination of initial conditions ($\alpha_1(0) = 0.20203$, $\dot{\alpha}_1(0) = -0.89034$, $\dot{\alpha}_2(0) = -0.17253$) is stable for small disturbance. In addition, by application of the cell mapping method that has been used in the several studies of passive dynamic walking,[5,6] we found that the model performs well in the concept of global stability. The allowable errors can be much larger than the results obtained by passive dynamic walkers with point foot. This can be inspected by the evaluation of the basin of attraction as shown in Fig. 7, which is the complete set of initial conditions that eventually result in cyclic walking motion. From Fig. 7(a), one can find that for passive dynamic walker with flat feet and compliant ankles, cyclic walking with parameter values in Table 2, emerges even if the initial step is nearly fourfold as large, e.g. $\{\alpha_1(0) = 0.8, \dot{\alpha}_1(0) = -2.3, \dot{\alpha}_2(0) = -0.8\}$.

3.2. Actively changing speed during stable walking

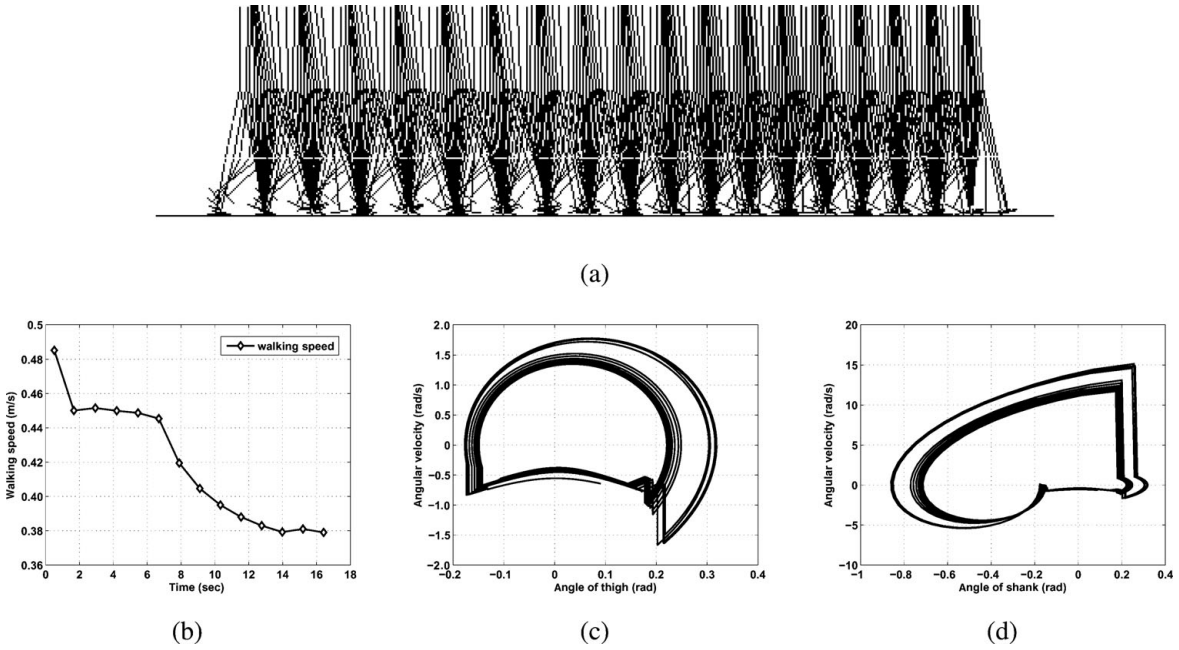
As one of the main limits of current studies on passive dynamic walking, how to control velocity of passive dynamic walkers is still a challenge. Mandersloot *et al.*[22] tried to control velocity of a simulated planar compass gait walker by using dynamic programming approach. Van Ham[21] attempted to use a range of compliances instead of a discrete number of compliances. Another try is to change the velocity of the walker simply by changing the set point to a new value.[23] Recently, several authors reported that proper actuation utilized on hip joint may improve the stability and



(a) (b)

Fig. 7. Basins of attraction: (a) the basin of attraction of the passive dynamic walking model with flat feet and ankle stiffness. The blue layers of points represent horizontal slices of a three-dimensional region of initial conditions that eventually result in the cyclic walking motion. The cyclic motion ($\alpha_1(0) = 0.20203$, $\dot{\alpha}_1(0) = -0.89034$, $\dot{\alpha}_2(0) = -0.17253$) is indicated with a red point, which is above one of the sample slices. Parameters values used in the analysis are obtained from Table I. (b) The basin of attraction of the passive dynamic walking model with point feet. The point-foot walker has the same mass and length parameters (except the foot length) with the flat-foot walker.

https://doi.org/10.1017/S0263574709005736 Published online by Cambridge University Press



(a) (b) (c) (d)

Fig. 8. Actively changing the speed during stable walking. The hip joint actuation changes in the way. The ankle stiffness k keeps the same when the walking speed alters. This result is obtained every 10 frames during a continuous walking simulation: (a) the stick diagram, (b) change of the average walking velocity, (c) the angular trajectory of the thigh and (d) the angular trajectory of the shank.

mobility of walking.[18,19] Hence, we evaluated the results of walking velocity control of the proposed model with controlled hip actuation. We also do some experiments on controlling the model on different walking velocities during continuous period. We change the magnitude of hip torque P to a different one instantaneously when the robot is walking stably with a constant velocity. Then the velocity changes gradually according to the new torques. At last, the model walks at another constant velocity stably. All the simulation results are based on the proposed two-dimensional model with parameter values listed in Table I. As mentioned above, our model is able to control the locomotion velocity by changing the hip actuation. At first, the passive walker steps forward from the very beginning to a relatively stable cycle gait. Then the hip joint actuation is set to decrease suddenly. It simulates the circumstance that one actively slow down the walking speed. Then the walker is actuated by a decreased actuation. Figure 8 shows the process. It is clear that the walker first achieves a stable walking velocity, then changes to a slower velocity where the stability maintains. The speed variance during this stable walking simulation is shown in Fig. 8(b). One can find that the model is sensitive to the changes of the hip torque, which can be used to vary walking speed of the model. Figure 8(c), (d) show the angular trajectory of the swing leg during walking. When the hip torque changes, the trajectories of swing shank and swing thigh transit from circle-like traces into smaller ones.

3.3. Adaptive walking on uneven terrains

Energy-conserving mechanisms, such as the tendinous tissues of the skeletal muscle, play an important role by improving adaptivity and efficiency in human walking and running. The mechanical energy stored in the elastic elements of muscle can be recovered as both kinetic and gravitational energy (spring-like bouncing mechanism).[17] By adding ankle stiffness, the adaptability of the proposed model is no surprise: the passive dynamic walker with flat feet and compliant ankles can achieve adaptive bipedal locomotion with larger disturbance on uneven terrain (see Fig. 9). Specifically in the simulation, we changed the level ground to an uneven floor. The hip joint actuation is the same with the simulation shown in Fig. 5. The passive walker is designed to walk on an uneven ground. To estimate the effects of walking with ankle stiffness independently, there is no learning process during adaptive walking. Figure 9 shows the result. The passive walker successfully performs a stable walking on the ground with -10 mm disturbance (1.4 % of the leg length) with no active control. Figure 9(b) and (c) show the trajectories of hip and knee during adaptive walking. Note that when the heel-strike event has not occurred as former step (first step to the new floor with disturbance), the walker performs a unstable phase in which the upper body fall backward. Since there is ankle stiffness in the ankle joint of the stance leg, the walker can overcome this unstable phase instantly. Then the stable walking maintains. It indicates that by adding proper ankle stiffness, passive dynamic walkers can perform adaptive locomotion on uneven terrain with no active control.

4. Discussions

Cyclic walking motion can be characterized by several observed parameters, such as step length notated as s_l, step frequency notated as s_f and walking speed notated as v. Here, step length is the distance the swing ankle travels over one step; step period is the time to take one step;

https://doi.org/10.1017/S0263574709005736 Published online by Cambridge University Press

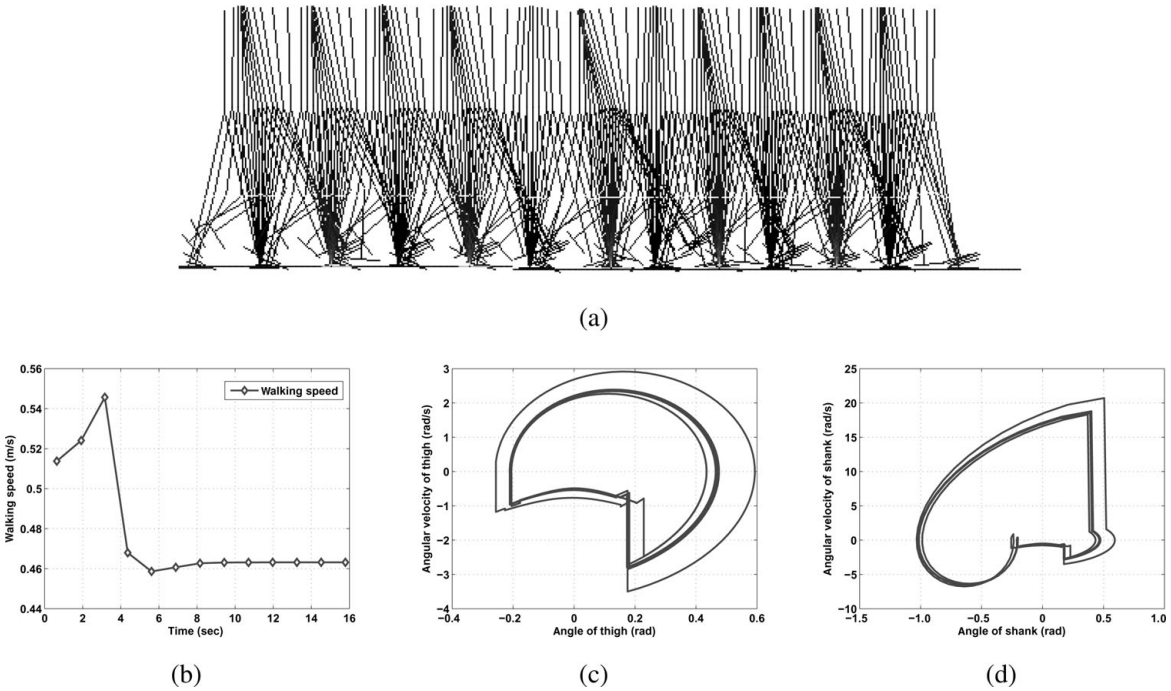


Fig. 9. Adaptive locomotion on uneven terrain. This result is obtained every 10 frames during a continuous walking: (a) the stick diagram, (b) and (c) the angular trajectories of the thigh and shank respectively.

and walking speed is step length/step period. Additionally, energetic efficiency notated as E_e, is another important gait characteristic. As mentioned in Section 2, the model has several parameters that are essential to the walking gait: the hip actuation (P), foot geometric parameter (l_f, r) and ankle stiffness (k). Together, they determine the observed parameters of periodic gaits. With a fixed set of mechanical parameters (mass and length) and joint stiffness, hip actuation can be used to control the walking velocity. For a fixed set of mechanical parameters (mass and length), the step length and step frequency of a stable waking gait are almost completely determined by the hip actuation and ankle stiffness. To understand the results observed in Section 3, we investigated the effects of different parameters of the proposed model. The ranges of different parameters are drawn from the cluster region described in Fig. 7, which lead to a stable cyclic walking motion.

4.1. Flat feet

Different from point feet[5,11,14] and round feet,[3,4,7] flat feet[2,12,15] will influence the passive dynamics of walking with heel-strike and toe-strike. The flat foot shape can be simply defined by two parameters, foot length l_f and foot-ankle ratio r. The foot geometric parameters l_f and r will influence the walking gait. An early research[15] indicated that given energy efficiency, as foot length increases from zero, walking speed increases until certain foot length is reached. Though the distance between the heel and ankle can affect the step length and frequency, for a fixed set of mass and length (except foot geometric parameters) and controllable parameters (P and k), there is no clear relation between this distance and the walking speed. Additionally, the relation between the distance from ankle to toe and the walking speed is linear. An increasing distance from ankle to toe will provide a higher walking speed if the model can keep stable. Furthermore, the relation between the distance from heel to ankle and the step frequency is also linear. A longer distance from heel to ankle will result in a lower step frequency. However, there is no clear relation between such distance and the step length. Contrarily, the distance from ankle to toe affects both the step length and step frequency linearly. A longer distance from heel to toe will lead to longer step length and higher step frequency.

It should be noted that these effects of flat feet are not unique to our model. In fact, Kwan and Hubbard[15] studied these same effects of foot geometric parameters extensively for the simplest walking model with flat feet to investigate optimal foot shape for passive dynamic walkers. However, for the range of foot lengths analysed here ($0 < l_f < 0.2$), actual r that works can be greater than 0.5. It indicated that the fore part of the foot has more influence on the speed and step length of passive dynamic walking with joint stiffness. Different from the effects of foot parameters on passive dynamic walkers with flat feet and stiff ankles (without ankle joints),[15] solutions of the proposed model still exist even if $r > 0.5$, e.g. $r = 0.57$.

Foot geometric parameters also influence the dynamic stability of the walker. Figure 10 shows the results. It is clear that as the foot length increased (within a certain range), the walker can handle larger ground disturbance. Furthermore, for a fixed foot length, it seems that there is an optimal foot-ankle ratio to obtain largest allowable ground disturbance. For example, when the foot length is 0.2, as the foot-ankle ratio increased, the walker obtains the largest allowable ground disturbance when foot-ankle ratio is about 0.4 (see the dashed line in Fig. 10). Different foot length may

https://doi.org/10.1017/S0263574709005736 Published online by Cambridge University Press

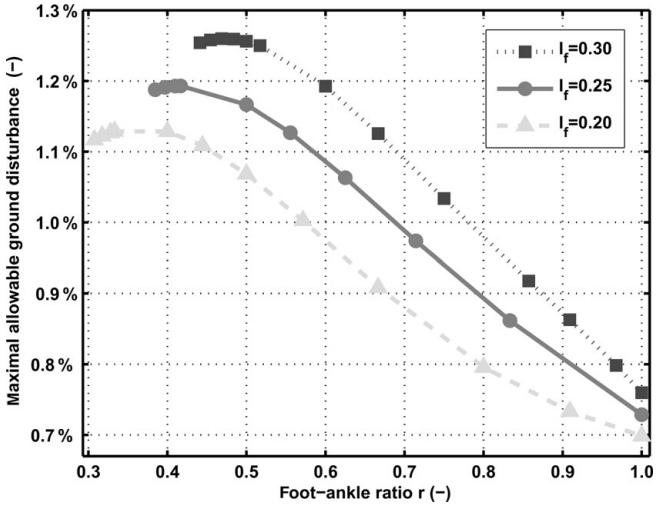


Fig. 10. Maximal allowable ground disturbance of the passivity-based bipeds with different foot-ankle ratio. All distances are normalized by leg length.

result in different optimal foot-ankle ratio. For example, the optimal foot-ankle ratio increases to 0.5 when foot length is 0.3 (see the solid line in Fig. 10).

4.2. Ankle stiffness

For a fixed set of mass, length and hip actuation, the bigger the ankle stiffness (k), the bigger the step length. As a result, the step frequency will decrease with an increasing k. Then we evaluated the effects of ankle stiffness (k) on the process of actively changing walking speed. The process is similar to the Fig. 8. We change the magnitude of hip torque P to a smaller one instantaneously when the robot is walking stably on a constant velocity, starting with corresponding fixed points of initial conditions that lead to cyclic motion. As shown in Fig. 11, under the same change of hip actuation, different k reveals different responses in walking velocity transition. It indicates that more compliance (relatively small k) results in more visible sensitivity to the change of hip torque. For example, when $k = 1.65$ Nm/rad, the model changes walking velocity from one stable value to a smaller one within 2 s. Contrarily, when $k = 35$ Nm/rad, it takes 6 s to achieve a stable walking after changing the magnitude of hip torque. If we change the compliant ankle to a stiff one (no ankle joint), only change the hip actuation will be the most inefficient way to change the walking speed. The time duration of the transition is over 15 s, which is much longer than the one with compliant ankles. Additionally, one can also find that under the same hip joint actuation, a relatively small k can achieve a faster stable walking. It indicates that more compliance (relatively small k) results in fewer collisional loses. Kwan and Hubbard[15] reported that for long period solutions, the point-foot model is the least efficient, the round-foot is the most efficient, and the flat-foot is in between. Short period solutions, however, show that flat feet can be more efficient than round feet. In our model of passive dynamic walking with compliance, the flat feet are connected to compliant ankle joints. A relatively big k can be considered as the similar case that the ankle is locked. As discussed above, flat-foot model with proper ankle stiffness added is more efficient than the flat-foot with stiff ankle.

Finally, we analyse the effects of ankle stiffness k on the stability of walking. Stability is usually quantified either by the basin of attraction, or by the eigenvalues of the Jacobian of the stride map. Similar to most of the current studies on stability analysis of passive dynamic walking, we use basin of attraction to quantify the stability, which corresponds to the size of a perturbation one can apply to the initial conditions. We select sections of basins of attractions which have the most stable points, as shown in

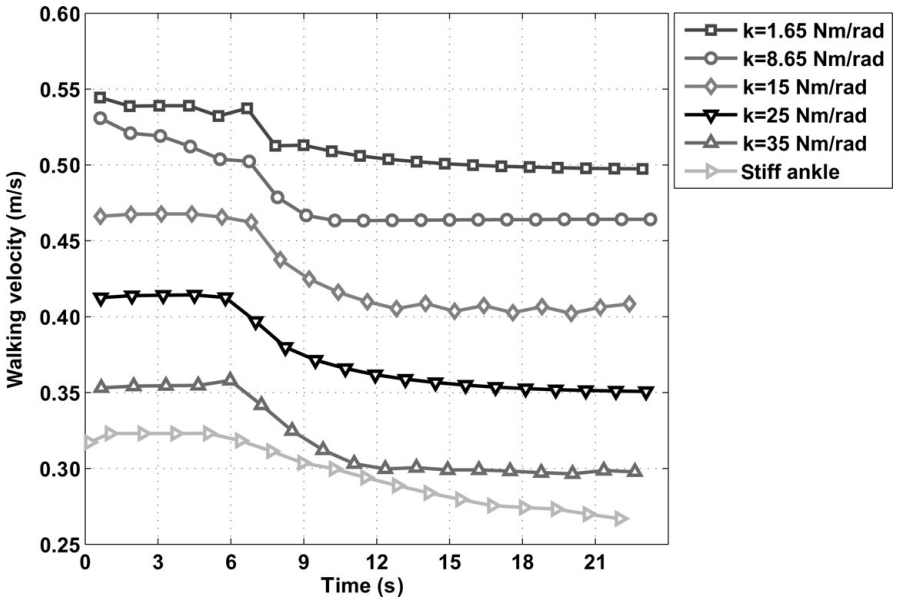
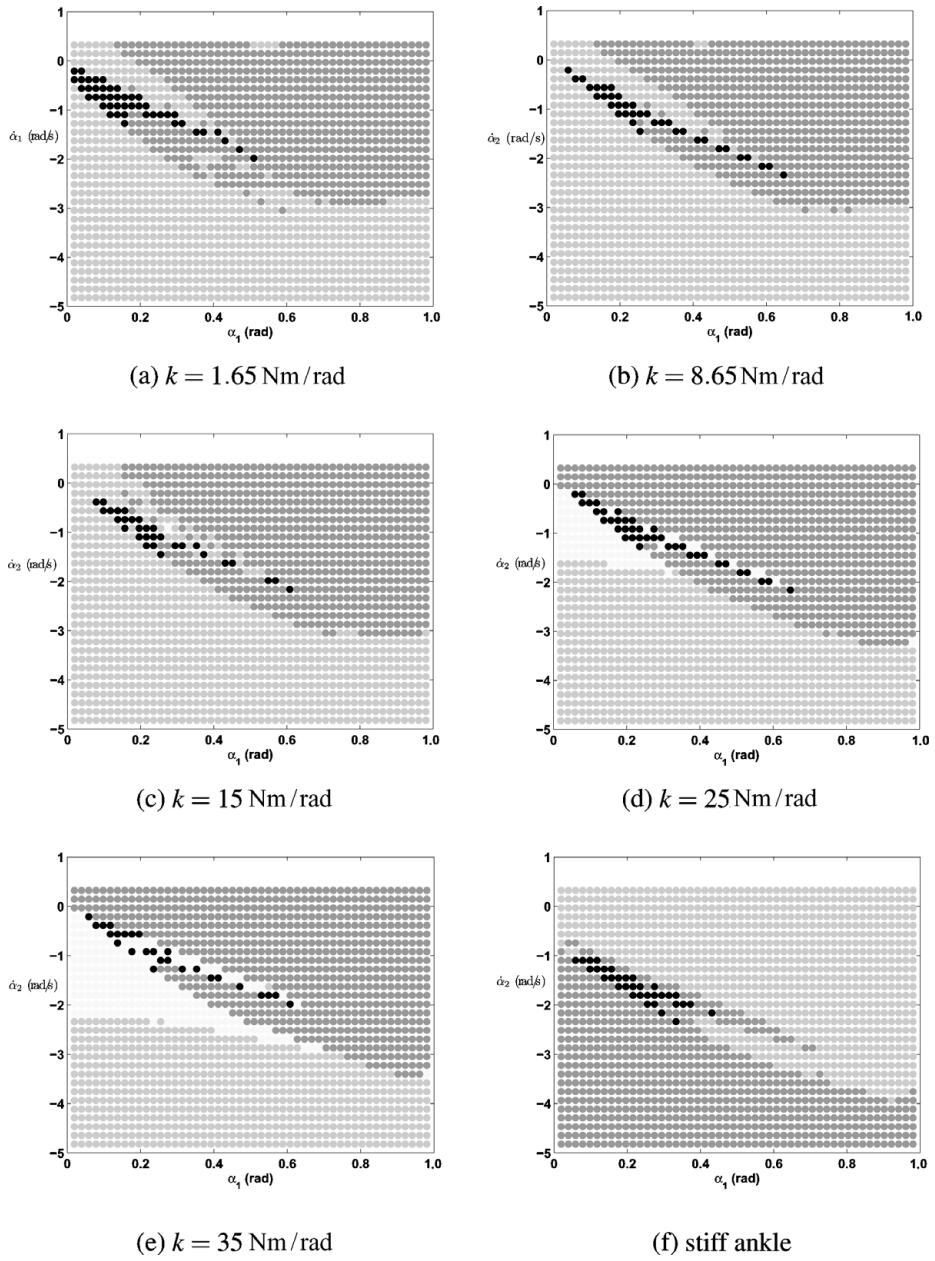


Fig. 11. Results of actively changing walking speed with the same hip actuation and different ankle stiffness (k varies).

https://doi.org/10.1017/S0263574709005736 Published online by Cambridge University Press



(a) $k = 1.65\,\mathrm{Nm/rad}$ (b) $k = 8.65\,\mathrm{Nm/rad}$

(c) $k = 15\,\mathrm{Nm/rad}$ (d) $k = 25\,\mathrm{Nm/rad}$

(e) $k = 35\,\mathrm{Nm/rad}$ (f) stiff ankle

Fig. 12. Sections from the basin of attraction for one of the fixed points at different k. The dark gray shading marks the points that lead to fall backwards. The light gray points indicate the initial conditions that result in running (both feet leave the ground at the same time). The black points are the initial conditions fall into a small neighbourhood of the fixed point, which lead to a stable cyclic walking motion. The yellow points are the ones that result in fall forwards.

Fig. 12. It indicates that the proper ankle stiffness may result in more stable dynamic walking (e.g. $k = 1.65$ Nm/rad), while an inappropriate compliant ankle (e.g. $k = 35$ Nm/rad) performs even worse than a stiff ankle in the view of walking stability. Figure 13 presents the results of adaptivity of ground disturbance of the model with different ankle stiffness. The relation between maximum allowable ground disturbance and ankle stiffness in nearly linear. Large ground disturbance needs a small ankle stiffness.

5. Conclusion

In this paper, we have demonstrated a bipedal locomotion model for passive dynamic walking with compliance added on the ankle joints. The model consists of an upper body, three-segment legs, hip joint actuation and passive ankle joints that are constrained by torsional springs. When the flat foot strikes the ground, there are two impulses, 'heel-strike' and 'toe-strike', representative of the initial impact of the heel and the following impact as the whole foot contacts the ground. By adding compliance on the passive joints, collisional loses can be reduced, while the adaptability and stability of dynamic walking can be increased. An appropriate combination of flat foot shape and ankle stiffness is essential for stability. The results indicated that for future passive dynamic walking robot applications, one may implement compliant ankle joints and shape-optimized flat feet to improve the mobility and

https://doi.org/10.1017/S0263574709005736 Published online by Cambridge University Press

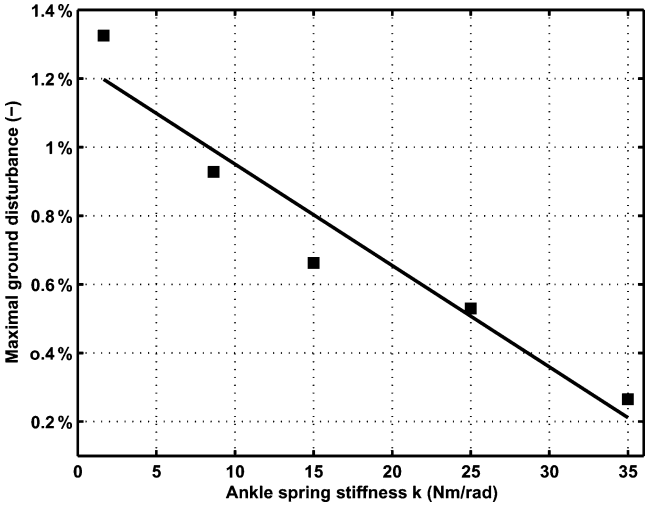


Fig. 13. Adaptability of ground disturbance of the proposed model with different ankle stiffness. All distances are normalized by leg length.

adaptability of walking towards more practical uses. It is convincing enough to commence the construction of a robot prototype with a similar design as proposed in the proposed model.

Acknowledgments

The authors would like to thank Wei Chen for contribution in simulation of the initial model. Dongjiao Lv contributed in the stick diagrams that visualize walking of the model. This work was supported by National Natural Science Foundation of China (No. 60404001 and No. 60274001) and the 985 Project of Peking University.

References

1. T. McGeer, "Passive dynamic walking," *Int. J. Robot. Res.* **9**, 68–82 (1990).
2. S. Mochon and T. A. McMahon, "Ballistic walking," *J. Biomech.* **13**(1), 49–57 (1980).
3. S. Collins, M. Wisse and A. Ruina, "A three-dimensional passive-dynamic walking robot with two legs and knees," *Int. J. Robot. Res.* **20**, 607–615 (2001).
4. S. Collins, A. Ruina, R. Tedrake and M. Wisse, "Efficient bipedal robots based on passive-dynamic walkers," *Science* **307**, 1082–1085 (2005).
5. M. Wisse, A. L. Schwab and F. C. T. Van der Helm, "Passive dynamic walking model with upper body," *Robotica* **22**, 681–688 (2004).
6. M. Wisse, D. G. E. Hobbelen and A. L. Schwab, "Adding an upper body to passive dynamic walking robots by means of a bisecting hip mechanism," *IEEE Trans. Robot.* **23**(1), 112–123 (2007).
7. M. Wisse, D. G. E. Hobbelen, R. J. J. Rotteveel, S. O. Anderson and G. J. Zeglin, "Ankle Springs Instead of Arc-Shaped Feet for Passive Dynamic Walkers," *Proceedings of the 2006 IEEE International Conference on Humanoids*, Genova, Italy (2006) pp. 110–116.
8. D. G. E. Hobbelen and M. Wisse, "Ankle Joints and Flat Feet in Dynamic Walking," *International Conference on Climbing and Walking Robots*, Madrid, Spain (2004).
9. D. G. E. Hobbelen and M. Wisse, "Ankle actuation for limit cycle walkers," *Int. J. Robot. Res.* **27**(6), 709–735 (2008).
10. E. Dertien, "Dynamic walking with dribbel," *IEEE Robot. Autom. Mag.* **13**(3), 118–122 (2006).
11. M. Garcia, A. Chatterjee, A. Ruina and M. Coleman, "The simplest walking model: Stability, complexity, and scaling," *ASME J. Biomech. Eng.* **120**, 281–288 (1998).
12. A. Ruina, J. E. A. Bertram and M. Srinivasan, "A collisional model of the energetic cost of support work qualitatively explains leg sequencing in walking and galloping, pseudo-elastic leg behavior in running and the walk-to-run transition," *J. Theor. Biol.* **237**(2), 170–192 (2005).
13. A. Ruina, "Passive-Dynamic Locomotion," *Fifth World Congress of Biomechanics Conference*, J. Biomech. (2006) vol. **39**(Sl), S359.
14. A. D. Kuo, "Energetics of actively powered locomotion using the simplest walking model," *ASME J. Biomech. Eng.* **124**, 113–120 (2002).
15. M. Kwan and M. Hubbard, "Optimal foot shape for a passive dynamic biped," *J. Theor. Biol.* **248**, 331–339 (2007).
16. H. J. Ralston, "Energy-speed relation and optimal speed during level walking," *Int. Z. Angew. Physiol.* **17**, 277–283 (1958).
17. M. Ishikawa, P. V. Komi, M. J. Grey, V. Lepola and G. Bruggemann, "Muscle-tendon interaction and elastic energy usage in human walking," *J. Appl. Physiol.* **99**, 603–608 (2005).
18. M. J. Kurz and N. Stergiou, "An artificial neural network that utilizes hip joint actuations to control bifurcations and chaos in a passive dynamic bipedal walking model," *Biol. Cybern.* **93**, 213–221 (2005).
19. E. Schuitema, D. Hobbelen, P. Jonker, M. Wisse and J. Karssen, "Using a Controller Based on Reinforcement Learning for a Passive Dynamic Walking Robot," *Proceedings of the IEEE-RAS International Conference on Humanoid Robots*, Tsukuba, Japan (2005) pp. 232–237.
20. S. Suzuki, K. Furuta and S. Hatakeyama, "Passive walking towards running," *Math. Comput. Modelling Dyn. Syst.* **11**(4), 371–395 (2005).
21. R. Van Ham, B. Vanderborght, B. Verrelst, M. Van Damme and D. Lefeber, "Controlled Passive Walker Veronica Powered by Actuators with Independent Control of Equilibrium Position and Compliance," *Proceedings of the 2006 IEEE International Conference on Humanoids*, Genova, Italy (2006) pp. 234–239.
22. T. Mandersloot, M. Wisse and C. G. Atkeson, "Controlling Velocity in Bipedal Walking: a Dynamic Programming Approach," *Proceedings of the 2006 IEEE International Conference on Humanoids*, Genova, Italy (2006) pp. 124–130.
23. G. Van Oort and S. Stramigioli, "Velocity Control of a 2D Dynamic Walking Robot," *Proceedings of the 26th Benelux Meeting on Systems and Control*, Lommel, Belgium (2007).
24. Q. Wang, J. Zhu and L. Wang, "Passivity-Based Three-Dimensional Bipedal Robot with Compliant Legs," *Proceedings of the SICE Annual Conference*, Chofu, Japan (2008).

https://doi.org/10.1017/S0263574709005736 Published online by Cambridge University Press